

Differential Effects of Nitrogen and Sulfur Deprivation on Growth and Biodiesel Feedstock Production of *Chlamydomonas reinhardtii*

Turgay Cakmak,^{1,2} Pinar Angun,¹ Yunus Emre Demiray,¹ Alper Devrim Ozkan,¹ Zeynep Elibol,^{1,3} Turgay Tekinay¹

¹Laboratory of Sustainable Technologies, UNAM Institute of Materials Science and Nanotechnology, Bilkent University, 06800 Ankara, Turkey; telephone: +90-312-290-3573; fax: +90-312-266-4365; e-mail: ttekinay@bilkent.edu.tr

²Faculty of Science, Department of Molecular Biology and Genetics, Istanbul Medeniyet University, 34730, Istanbul, Turkey

³Faculty of Arts and Sciences, Department of Biology, Kırkkale University, 71450, Kırkkale, Turkey

ABSTRACT: Biodiesel production from microalgae is a promising approach for energy production; however, high cost of its process limits the use of microalgal biodiesel. Increasing the levels of triacylglycerol (TAG) levels, which is used as a biodiesel feedstock, in microalgae has been achieved mainly by nitrogen starvation. In this study, we compared effects of sulfur (S) and nitrogen (N) starvation on TAG accumulation and related parameters in wild-type *Chlamydomonas reinhardtii* CC-124 mt(-) and CC-125 mt(+) strains. Cell division was interrupted, protein and chlorophyll levels rapidly declined while cell volume, total neutral lipid, carotenoid, and carbohydrate content increased in response to nutrient starvation. Cytosolic lipid droplets in microalgae under nutrient starvation were monitored by three-dimensional confocal laser imaging of live cells. Infrared spectroscopy results showed that relative TAG, oligosaccharide and polysaccharide levels increased rapidly in response to nutrient starvation, especially S starvation. Both strains exhibited similar levels of regulation responses under mineral deficiency, however, the degree of their responses were significantly different, which emphasizes the importance of mating type on the physiological response of algae. Neutral lipid, TAG, and carbohydrate levels reached their peak values following 4 days of N or S starvation. Therefore, 4 days of N or S starvation provides an excellent way of increasing TAG content. Although increase

in these parameters was followed by a subsequent decline in N-starved strains after 4 days, this decline was not observed in S-starved ones, which shows that S starvation is a better way of increasing TAG production of *C. reinhardtii* than N starvation.

Biotechnol. Bioeng. 2012;109: 1947–1957.

© 2012 Wiley Periodicals, Inc.

KEYWORDS: biodiesel; *Chlamydomonas reinhardtii*; microalgae; nitrogen starvation; sulfur starvation; triacylglycerol

Introduction

Microalgae are planet's primary biological CO₂/O₂ converters and they are a potential source of valuable products such as pigments, vitamins, and biofuel feedstock. Today, microalgae are used in a wide range of areas; such as wastewater treatment, production of protein-rich food and feed additives, high value added compounds, and biofuel (Demirbas, 2008; Doan et al., 2011). Limited fossil fuel reserves of the earth have been rapidly depleting and there is an increasing need for renewable energy sources, specifically biofuels (Balat, 2008). While industrially important potential sources of biofuels include various vascular plants such as sugarcane, palm, corn, and soybeans, microalgae have emerged as a promising third-generation biofuel source and present a possible solution to our energy problems (Moazami et al., 2011; Rodolfi et al., 2009). However, knowledge on increasing biofuel feedstock [such as triacylglycerol (TAG) and biohydrogen production] level of microalgae needs to be improved for more efficient usage.

TAG is an ester of three fatty acids and glycerol. All eukaryotic organisms have the ability to synthesize TAG, which is the main constituent of vegetable oil, algal lipid bodies, and animal fats. In microalgae, changes in

Correspondence to: T. Tekinay

Contract grant sponsor: Turkish Ministry of Agriculture and Rural Affairs General Directorate of Agricultural Research

Contract grant number: TAGEM-10/AR-GE/26

Contract grant sponsor: State Planning Organization of the Republic of Turkey

Received: 26 October 2011; Revision received: 18 January 2012;

Accepted: 6 February 2012

Accepted manuscript online 21 February 2012;

Article first published online 2 March 2012 in Wiley Online Library

(<http://onlinelibrary.wiley.com/doi/10.1002/bit.24474/abstract>)

DOI 10.1002/bit.24474

environmental conditions such as temperature and light intensity or nutrient media characteristics such as iron supplementation and urea, nitrogen, or phosphorus limitation are known to enhance lipid accumulation (Converti et al., 2009; Dean et al., 2010; Hsieh and Wu, 2009; Liu et al., 2008; Zemke et al., 2010). With the abilities to grow both phototrophically and heterotrophically, respond rapidly to environmental stress with pronounced metabolic changes and a known genome sequence (Merchant et al., 2007), *Chlamydomonas reinhardtii* in particular is an attractive model for investigation of a wide range of biological functions, including starch metabolism (Ball et al., 1990), lipid metabolism (Ball et al., 1991), flagella formation (Marshall, 2008), photosynthesis (Rochaix, 2002), synthesis of bioenergy carriers (Kruse et al., 2005), or nutrient stress (Moellering and Benning, 2010). While a large volume of literature is present on starch biosynthesis; TAG metabolism is relatively less documented in microalgae, including *C. reinhardtii*. As TAG production is vital to the use of microalgae as biofuel, investigation of its synthesis mechanism is of considerable interest.

Nutrient deficiency is known to induce a wide variety of cellular response mechanisms in living organisms. Increase in lipid accumulation in different *C. reinhardtii* mutants during nitrogen (N) limitation and increased anaerobic H₂ production under sulfur (S) deprivation were previously reported (Dean et al., 2010; Morsy, 2011). However, to our knowledge, comparison of the effects of N and S starvation on TAG accumulation and related parameters in microalgae has not been studied to date. In this study, our aim was to determine and compare the effects of N and S starvation on biodiesel feedstock production levels and evaluate the importance of mating type on the nutrient starvation response of *C. reinhardtii*.

Materials and Methods

Strains, Culture Conditions, and Experimental Outline

The CC-124 wild-type mt(−) 137c and CC-125 wild-type mt(+) 137c strains were obtained from the Chlamydomonas Resource Center (www.chlamy.org). Cells were grown at 23°C under continuous light (150 μmoles photons m^{−2} s^{−1}) in liquid cultures on a rotary shaker (120 rpm). Standard tris-acetate-phosphate (TAP) medium, which includes acetate (17.4 mM) as carbon source and tris-base (20 mM) as buffering, was described previously (Harris, 1989). The starting cell density was approximately 2.86 × 10⁴ cells mL^{−1} in all groups. For N starvation studies, cells were centrifuged at 2,000g for 3 min at room temperature; cell pellets were kept and washed twice in TAP medium without N (TAP-N). Pellets were then resuspended in TAP-N medium and cells were grown under constant light on a rotary shaker. The same procedure was followed for S starvation studies using TAP medium without S (TAP-S). Each treatment consisted of triplicate flasks. Initial pH values in all media were set to 7

before algal cell inoculation and pH value of the media was checked every 24 h during 7 days of incubation period. Initial pH values in the media did not deviate more than 5% during 7 days of incubation period. Cell growth and size were monitored by cell counts with a hemocytometer using lugol solution (Sigma) and Image-J, a java-based image processing program developed at the National Institutes of Health (Collins, 2007). Total cell biovolume was calculated using the equation “B = CV,” in which B is the total biovolume, C is cell count, and V is cell volume. For relative dry weight measurement, enough volume of culture media including 1 × 10⁹ cells were centrifuged at 3,000 rpm for 5 min, pellet was air-dried for 5 min, weighed and incubated at 80°C for 48 h, thereafter cells were re-weighed. Cells from all experimental groups (CC-124 and CC-125 strains grown in TAP, TAP-N, and TAP-S media) were harvested every 24 h for 7 days following N and S starvation.

Chlorophyll, Carotenoid, and Protein Quantification

For chlorophyll a,b,c and carotenoid determination, protocol described by (Jeffrey and Humphrey, 1975) was followed with some modifications. Frozen cells (1 × 10⁷ cells) were re-suspended with 500 μL of 90% acetone, incubated by mixing for 15 min and centrifuged at 15,000 rpm for 5 min. The supernatant was then loaded in a 96-well plate. The absorbance of the supernatant at 470, 630, 647, 664, and 750 nm wavelengths were collected and calculation determination of chlorophyll a,b,c and carotenoid contents were performed following the formulae given by (Jeffrey and Humphrey, 1975) and (Lichtenthaler, 1987). Total chlorophyll results were presented as a sum of chlorophyll a,b, and c.

Protein extraction was performed according to (Weis et al., 2002) with some modifications. Frozen cell pellets were re-suspended in lysis buffer (50 mM Tris-HCl pH 8.0, 2% SDS, 10 mM EDTA, protease inhibitor mix), subjected to sonication (3510E-DTH, Branson) for 1 min at 60% power (≈7 W/pin), frozen in liquid nitrogen for 1 min, thawed and centrifuged at 13,000g for 20 min at 4°C. The supernatant was then used for protein determination with Bradford method (Bradford, 1976).

Quantification of Starch and Neutral Lipids

Neutral lipid-staining using Nile Red was performed essentially as described previously (Elsey et al., 2007). Approximately, 29.3 × 10⁴ cells mL^{−1} were stained with 22 μL of 7.8 × 10^{−5} M Nile Red (9-diethylamino-5H-benzo[a]phenoxazine-5-one) (Invitrogen) dissolved in acetone (final concentration 0.26 μM), left to incubate on a shaker for 15 min under dark conditions and washed twice with TAP-N or TAP-S media. Relative fluorescence intensity of Nile Red staining was quantified on a fluorescence spectrometer (SpectraMax M5, MDS Analytical Technologies, Sunnyvale, CA) using 490 nm excitation and 585 nm emission

values. For starch-staining, cells were stained with 0.02% Safranin O (Sigma) and relative fluorescence intensity of Safranin O staining was quantified using 435 nm excitation and 480 nm emission wavelengths (Klut et al., 1989). Total neutral lipid levels were also determined gravimetrically from 1×10^9 cells using a method of Bligh and Dyer (1959). The lipids were extracted and separated with a final solvent ratio of chloroform:methanol:water of 1:1:0.5. In order to collect neutral lipids, the chloroform layer was transferred into a pre-weighed vial, evaporated in a water bath (30°C) using a rotary evaporator, dried in a vacuum oven (Model No:2255; VacuCell); then, vials were reweighed.

Confocal Imaging of Live Cells

Cells were stained with Nile Red (5 µg/mL final concentration; Invitrogen) as described by (Wang et al., 2009). Images were acquired using an LSM 510 confocal microscope (Carl Zeiss) and a Plan Apo 63 oil immersion objective lens with a numerical aperture of 1.40–0.60. The Nile Red signal was captured using a laser excitation line at 488 nm, and the emission was collected between 560 and 600 nm; chlorophyll fluorescence was captured using a laser excitation line at 633 nm, and the emission was collected at 650 nm. Images were merged and pseudo-colored using ZEN 2008 CLSM user interface software. For three-dimensional imaging, Z stacks through an entire cell were acquired at 0.2- to 0.4-µm intervals, and each set was computationally projected using ZEN 2008.

Fourier Transform Infrared Spectroscopy (FTIR)

A 1.3 mL sample was aliquoted from each replicate flask for each experimental group, centrifuged, the supernatant removed and the cells re-suspended in 70 µL of distilled water, 30 µL of which was then deposited on a 96-well silicon microplate, and oven-dried at 42°C for 45 min (Dean et al., 2010). The plate was placed in a micro-well plate accessory and FTIR spectra were collected using a Nicolet 6700 Research FT-IR Spectrometer (Thermo Scientific). Spectra were collected over the wavenumber range 4,000–600 cm^{-1} . Each sample was analyzed in triplicate. Spectra were baseline corrected using the automatic baseline correction algorithm and were scaled to the amide I peak. In order to visualize the decrease of bands independent from the cell number, the information obtained was analyzed on a per cell level.

Statistical Analysis

Final data in this article are the mean values of at least three separate samples collected at two different times ($n = 6$). The fluctuation ranges of each point on the figures were not indicated to avoid complication of the figures. Statistical analysis was accomplished by means of average values,

standard errors, and *t*-test (two tails, pair type) with the significance criterion of 0.05, 0.01, or 0.001.

Results and Discussion

Effects of Nutrient Starvation on Algae Growth

In order to define and compare the effects of S and N starvation on algae growth, we performed cell count and volume measurements during 7 days of nutrient deprivation. Cells were incubated in 50 mL of culture media with a starting cell density of approximately 2.86×10^4 cells/mL. Control and S-starved CC-124 cells entered stationary phase with a maximum of 1227×10^4 and 422×10^4 cells on day 4 while N-starved cells entered stationary phase on the first day with 209×10^4 cells (Fig. 1a and b). CC-125 control and S-starved cells entered stationary phase with a maximum of $1,050 \times 10^4$ and 534×10^4 cells on day 6 while N- and S-starved cell density reached their highest level with a maximum of 364×10^4 cells on day 4 (Fig. 1a and b).

Initial cell volumes in CC-124 and CC-125 were 87.8 ± 19.1 and $103.9 \pm 13.4 \mu\text{m}^3/\text{cell}$, respectively. Cell volume increase in response to S deprivation was much higher than the increase under N deprivation in both strains throughout 7 days of nutrient starvation. Maximum increase in cell volume was observed 4 days after nutrient starvation with 2.9- to 6.1-fold and 1.7- to 5.8-fold; and this increase was followed by a subsequent decline resulting in a final increase of 1.8- to 4.4-fold and 1.6- to 4.1-fold in N- or S-starved CC-124 and CC-125 strains, respectively, during 7 days of nutrient starvation (Fig. 1c and d). As N and S starvation gave highest increases in cell biovolume on 4th day of incubation, we wanted to check possible changes in relative dry weight of cells at this time point (Table I). Relative dry weight measurement revealed that 4 days of N and S starvation causes approximately 31.8% and 27.4%, and 23.3% and 20% decrease in CC-124 and CC-125 strains when compared to those of respective controls (Table I). Total biovolume was gradually reduced by 62.6% and 54.6% in N-starved CC-124 and CC-125 cells, respectively, by day 7. However, it increased up to 2.2- and 3.1-fold by day 4; and this increase was followed by a subsequent decline in S-starved CC-124 and CC-125 cells (Fig. 1e and f).

Nutrient starvation triggers a wide range of responses through different mechanisms in microalgae. Some of these responses may result in increased lipid production and thus increased biodiesel production. Decline in microalgal growth rate and increase of cell volume have previously been reported as a consequence of N and S starvation (Degrenne et al., 2011; Young and Beardall, 2003). However, some studies reported that algal growth rate and cell volume may both decrease upon N starvation (Lynn et al., 2000). Our study show that microalgal cell division was strictly precluded, relative dry biomass decreased, and total biovolume was reduced in despite of the increases in cellular

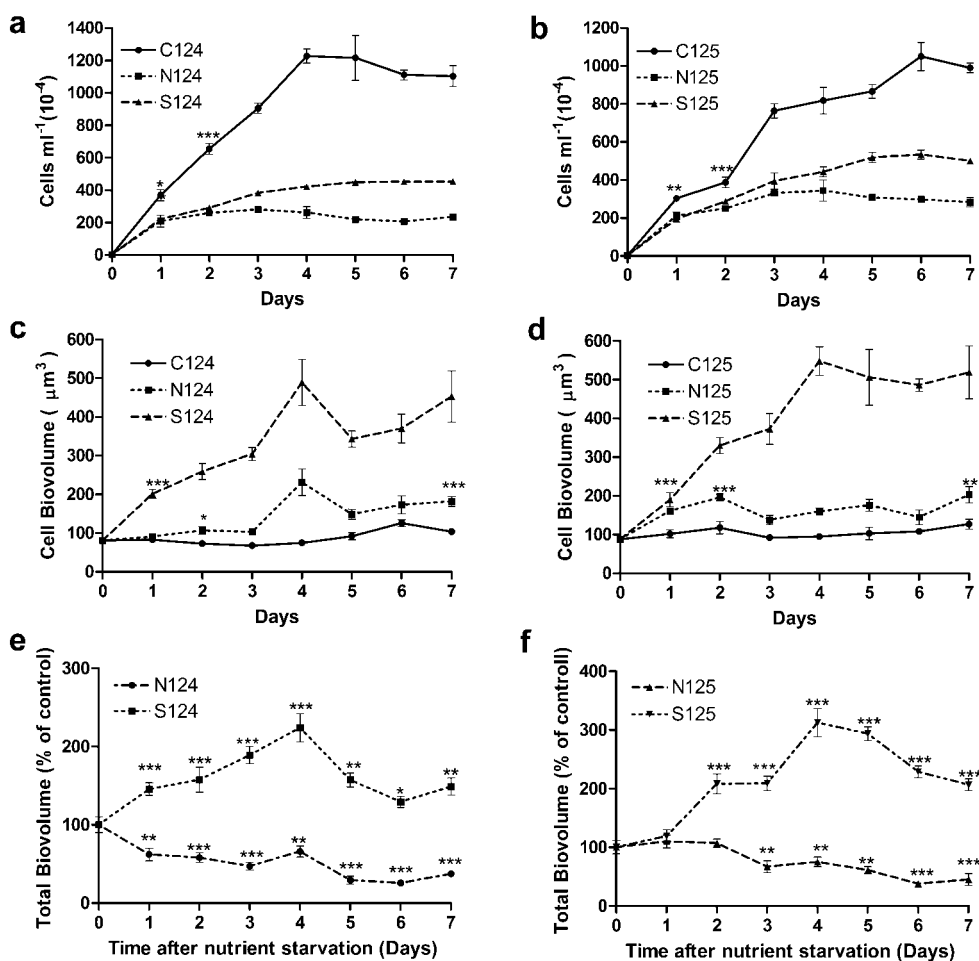


Figure 1. Changes in cell counts (a,b), cellular volume (c,d), and total biovolume (e,f) in response to N or S deprivation. For all data sets, each point represents the mean (\pm SE) of at least three replicate culture flasks. Symbols (*, **, ***) denote significance evaluated across all experiments ($P < 0.05^*$, 0.01^{**} , or 0.001^{***}). Except for total biovolume, significance signs were not indicated in each point to avoid complication of the figures. C124 and C125 indicate control cells, N124 and N125 indicate N-starved cells, S124 and S125 indicate S-starved CC-124 and CC-125 cells, respectively.

biovolume under N deprivation. On the other hand, S starvation-based decrease of cell growth and relative dry biomass is lower and increase of cell volume is higher than N starvation resulting with the increased total biovolume which would also be an important factor for selection of an approach for biodiesel production strategies as cytoplasmic lipid accumulation is thought to be related to the volume of a microalga (Wang et al., 2009).

Changes in Chlorophyll and Carotenoid Content

For an efficient utilization of carbon sources and to meet their energy demands, microalgae need to keep chlorophyll and carotenoid levels in a balance. Under normal conditions, chlorophyll levels of the CC-124 and CC-125 strains were 4.88 and 5.48 times higher than carotenoid levels on average (Fig. 2a and b). However, there was a rapid and

Table I. Relative dry weight and total neutral lipid levels (on a dry weight basis) of 4-day nutrient-starved CC-124 and CC-125 strains.

	124C	124N	124S	125C	125N	125S
Dry weight (%)	12.1 \pm 1.1	8.3 \pm 0.7	9.3 \pm 0.6	11.4 \pm 0.9	8.2 \pm 1.1	9.1 \pm 0.7
Total neutral lipid (%)	16.8 \pm 2.2	39.8 \pm 5.5	37.6 \pm 4.1	14.2 \pm 1.2	41.4 \pm 3.7	39.7 \pm 5.1

Approximately 1×10^9 cells were used for each measurement.

gradual decrease in chlorophyll:carotenoid ratio in response to nutrient starvation (Fig. 2a and b). Chlorophyll content decreased and carotenoid content increased rapidly even after 1 day of nutrient starvation. Decrease in chlorophyll content was higher in N-starved cells than those of S-starved ones. The decrease in total chlorophyll content was approximately 64–60% and 76–63% on first day and lasted with 78–65% and 89–46% during 7 days of N–S starvation in CC-124 and CC-125 cells (Fig. 2c and d), respectively. Intriguingly, N starvation-based carotenoid increase was higher in CC-124 but lower in CC-125 strain than that of S starvation. Carotenoid content increased up to 634% or 427% on day 5 followed by a subsequent decline, resulting with 514% and 183% increase after 7 days of N or S starvation in CC-124. However, N or S starvation caused a gradual increase in carotenoid levels in CC-125, increasing

from an initial value of 135–228% to a final value of 260–442% after 7 days of N and S starvation (Fig. 2e and f).

Restricted ability to maintain the photosynthetic functions stemming from decrease in chlorophyll content in response to N and S starvation have previously been reported (Young and Beardall, 2003; Zhang et al., 2002). Under such circumstances, some algae accumulate massive amounts of carbon in the form of carotenoids, starch, and lipids (Thompson, 1996). It has been suggested that the accumulation of carotenoid under stress conditions represents a mechanism to protect algal cells from damage by light (Ledford and Niyogi, 2005). Our results demonstrate that N and S deprivation causes a decrease in chlorophyll levels and increase of carotenoid content. However, CC-124 and CC-125 strains gave different regulation responses to N and S starvation. In particular,

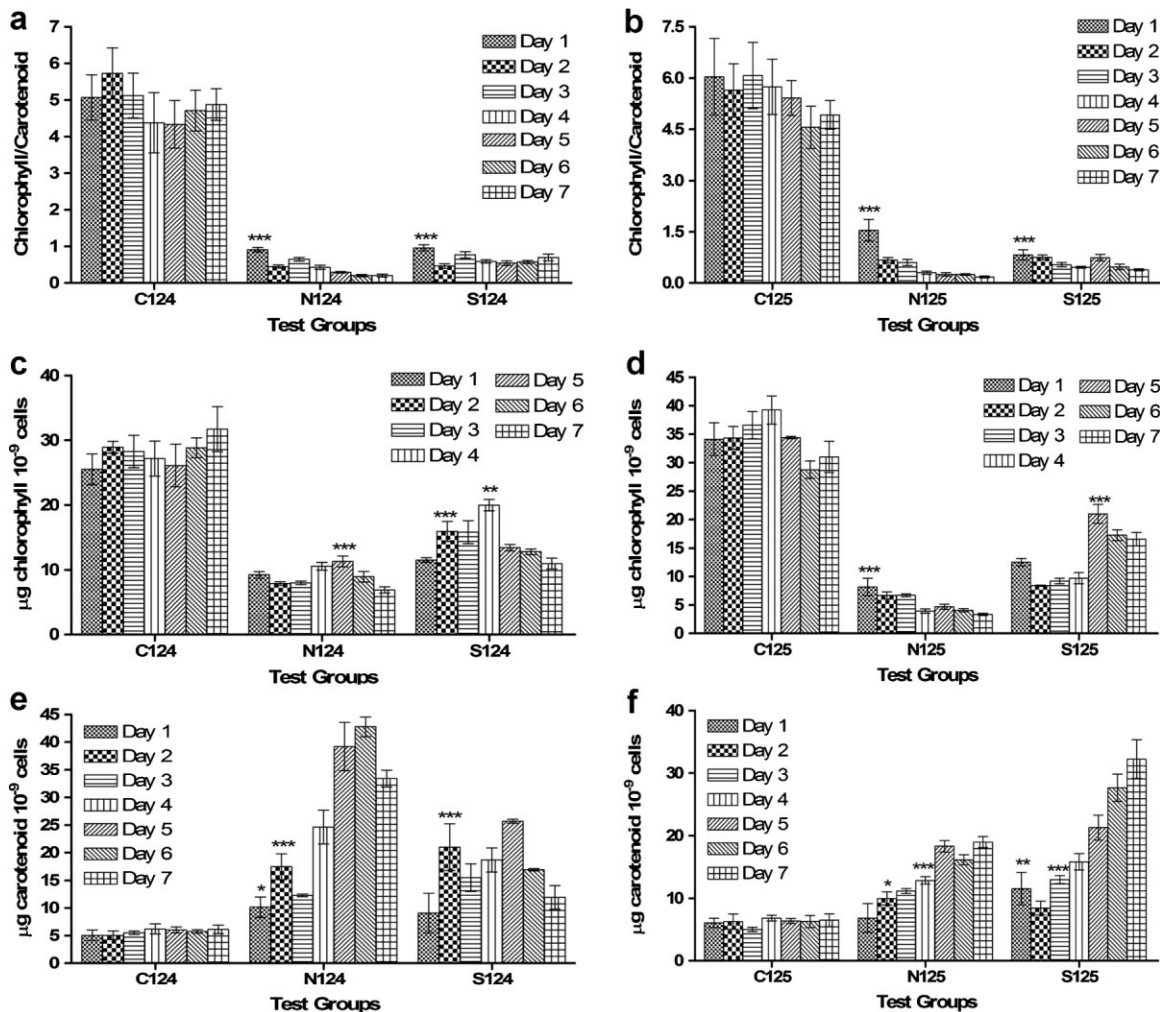


Figure 2. Changes in chlorophyll (a,b), carotenoid (c,d), and chlorophyll/carotenoid (e,f) content of CC-124 (a,c,e) and CC-125 (b,d,f) strains in response to N or S deprivation. For each treatment and time point chlorophyll and carotenoid content were quantified from 1×10^7 cells per sample. Total chlorophyll content was presented as a sum of Chl a, b, and c. Each data point is the mean (\pm SE) of at least three samples. Symbols (*, **, ***) denote significance evaluated across all experiments ($P < 0.05^*$, 0.01^{**} , or 0.001^{***}). The fluctuation ranges of each point on the figures were not indicated to avoid complication of the figures. C124 and C125 indicate control cells, N124 and N125 indicate N-starved cells, S124 and S125 indicate S-starved CC-124 and CC-125 cells, respectively.

S starvation-based increase in carotenoid content was lower in CC-124, but higher in CC-125 than that of N starvation. This difference may be related to the mating type of CC-124 (mt⁻) and CC-125 (mt⁺).

Changes in Protein, Total Neutral Lipid, and Starch Levels

Total soluble protein concentration in the algal samples decreased drastically in response to nutrient starvation. An 82% decrease in protein content was observed after 1 day of nutrient deprivation and a decrease of over 92% was observed by day 7 (Fig. 3a and b). On the other hand, total neutral lipid and starch levels increased inversely to the decrease in protein content. Maximum increase of total lipid content was reached 4 days after nutrient starvation in both

strains studied. Increase in lipid content was 240% and 258% in CC-124 and 165% and 302% in CC-125 in response to N and S starvation, respectively (Fig. 3c and d). Besides fluorescence Nile Red determination, increase in neutral lipid content of 4 days N- and S-starved cells was also supported by analytical measurements. Neutral lipid content of 4 day N- and S-starved CC-124 cells showed approximately 136% and 123%, CC-125 cells showed 190% and 172% increase when compared to their respective controls. Starch levels increased rapidly after nutrient starvation. Maximum increase of starch content was reached 3 days after nutrient starvation in both strains: 706% and 713% in CC-124, 490% and 571% in CC-125 in response to N and S starvation, respectively (Fig. 3e and f). In general, decrease in protein content was followed by a simultaneous increase in lipid and starch content in both strains upon exposure to nutrient starvation. Strikingly, S deprivation

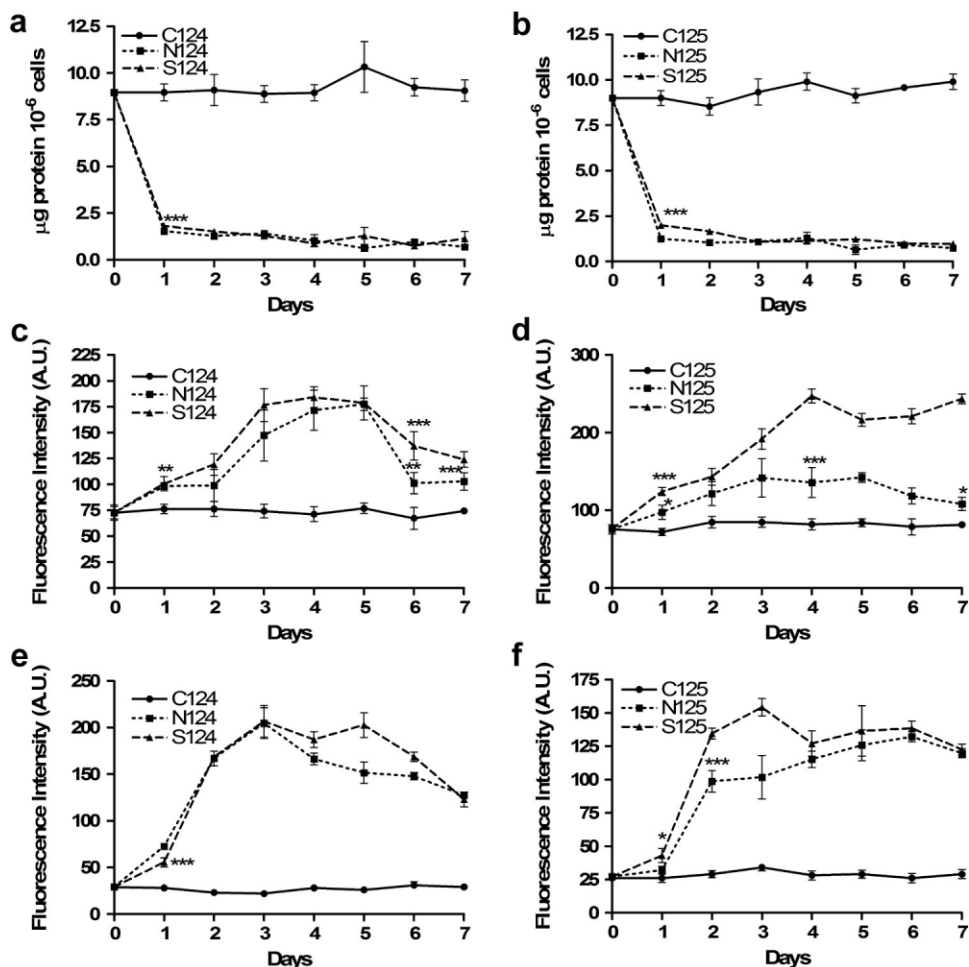


Figure 3. Total soluble protein (a,b), total lipid (c,d) and starch content (e,f) of CC-124 (a,c,e) and CC-125 (b,d,f) strains in response to N or S deprivation. For each treatment and time point the fluorescence emission of Nile Red (lipid) and Safranin O (starch), and protein absorbance values were quantified from 1×10^6 cells per sample. Each data point is the mean (\pm SE) of at least six samples. Symbols (*, ***, ****) denote significance evaluated across all experiments ($P < 0.05$, 0.01 , or 0.001). The fluctuation ranges of each point on the figures were not indicated to avoid complication of the figures. N', nitrogen-starved cells. S', sulfur-starved cells. C124 and C125 indicate control cells, N124 and N125 indicate N-starved cells, S124 and S125 indicate S-starved CC-124 and CC-125 cells, respectively.

caused higher lipid and starch accumulation than N deprivation. Moreover, starch content increment was faster and higher than increase in lipid content in response to nutrient starvation.

Potential competition between synthesis of lipid derivatives and carbohydrates is an important factor when deciding optimal biofuel production strategies. If starch metabolism interferes with lipid production in N- or S-starved algae, then disabling starch synthesis may be a simple and effective method to increase net lipid production. Increased lipid synthesis on a dry weight basis has been reported in *C. reinhardtii* mutants with defective starch synthesis machinery (Li et al., 2010), though lipid content was not investigated on a per cell basis. Another starchless *C. reinhardtii* mutant was determined to display 1.5- to 2.0-fold increase in lipid content per cell, suggesting that lipid and starch syntheses do antagonize each other (Wang et al., 2009). However, high production of both starch and oils has been recently reported from *C. reinhardtii* and this result is inconsistent with the competition hypothesis (Work et al., 2010). Our studies show that both starch and lipid content increased greatly in response to nutrient starvation. However, maximum increase in starch content was threefold higher than lipid content increment. This may indicate that *C. reinhardtii* wild-type strains first accumulate starch and that lipid synthesis is induced together with carbohydrate accumulation under nutrient starvation.

Confocal Microscopy Analysis

Ellipsoid-shaped cells (corresponding to the normal morphology of *C. reinhardtii* cells) were gradually replaced with larger and spherical cell shapes in the initial stages of N and S deprivation (Fig. 4), followed by cell mass reductions after longer nutrient deprivation. TAG are stored in cytosolic lipid bodies in microalgae which may account for the increase in cell volume we observed. Indeed, three dimensional pictures taken from day 4 of N- or S-starved cells show that the amount and volume of cellular cytosolic lipid bodies are higher in S-starved strains than that of N-starved ones. This suggests that increase of the density and volume of lipid bodies is directly related to increase in biovolume of the unicellular alga *C. reinhardtii*.

Relative Triacylglycerol, Oligosaccharide, and Polysaccharide Detection by FTIR

Quantification of biomolecules by FTIR is a relatively new approach. Following spectrophotometric detection of neutral lipid and starch levels, we performed FTIR measurement for detection of polysaccharide, oligosaccharide, and TAG levels. Infrared spectra were recorded in transmission mode with 128 scans in the range 4,000–600 cm^{-1} . The bands were assigned to specific molecular groups on the basis of biochemical standards and published studies as previously described (Movasaghi et al., 2008).

Bands were attributed to asymmetric stretching vibration of CH_2 of acyl chains (2,922 cm^{-1}); Amide I absorption (1,652 cm^{-1}); C–N stretching and CHN bending vibrations of amides from proteins (Amide II, 1,544 cm^{-1}); asymmetric CH_3 bending of the methyl groups of proteins (1,449 cm^{-1}); δCH_3 stretching of C–O groups (1,380 cm^{-1}); PO_2^- asymmetric bonds associated with phosphorus compounds (1,260 cm^{-1}) and PO_2^- symmetric stretching of phosphodiester (1,075 cm^{-1}). Three bands were of particular interest which were attributed to ester group (C=O) vibration of triglycerides (1,744 cm^{-1}), membrane-bound oligosaccharide C–OH bond (1,145 cm^{-1}), and C–O stretching frequencies coupled with C–O bending frequencies of the C–OH groups of polysaccharide (1,045 cm^{-1}).

According to the total soluble protein determination results, protein concentration decreased by up to 93% in response to nutrient deprivation. However, FTIR spectra levels of amide I band obtained from control cells did not at any time deviate more than 32%, therefore, we chose the amide I band for normalization of the FTIR spectra and ratio determination. Relative TAG, polysaccharide, and oligosaccharide contents were determined by calculating the ratio of TAG (1,744 cm^{-1}), polysaccharide (1,045 cm^{-1}), and oligosaccharide bands (1,145 cm^{-1}) to the amide I band (1,652 cm^{-1}). For each data set, we calculated fold-change values compared to their respective controls. Fold changes and standard errors were estimated by fitting a linear model for each time point and empirical Bayes smoothing was applied to the standard errors for all samples studied. Ratios of TAG, polysaccharide and oligosaccharides to Amide I of control samples were arbitrarily assigned a value of 1, independently for each time point. Increases in TAG, polysaccharide and oligosaccharide contents of nutrient-starved samples were defined as values displaying “—fold increase” in ratios of interested bands to Amide I band (Fig. 5). On the other hand, variations in the sample preparation process, such as the thickness of dried sample layers on microtiter plates, is a crucial point and can lead to nonlinear deviations. The distribution of dried cells on the microtiter plates is usually inhomogeneous. However, as a result of the drying procedure during sample preparation, all cells collapse forming a thin film of biomolecules on the sample holder (silica plate). Thus, the thickness of this layer is crucial for the absorbance through the sample, rather than the optical property of the microalgae cells itself. In the present study, we minimized deviations due to attenuation artifacts by applying limited cell numbers forming a sample film which yielded a maximum amide I absorption value of 0.2–0.3.

Infrared spectroscopy results showed that relative TAG, oligosaccharide, and polysaccharide levels increased rapidly in response to nutrient starvation. Starting with an initial increment of approximately 5- or 3.1-fold in CC-124 and 2.3- or 2.1-fold in CC-125, relative TAG content reached its maximum level with 6.9- or 15.3-fold in CC-124 and 29.1- or 16.5-fold in CC-125 after 4 days of N or S starvation, respectively (Fig. 5a). However, the increase in TAG content

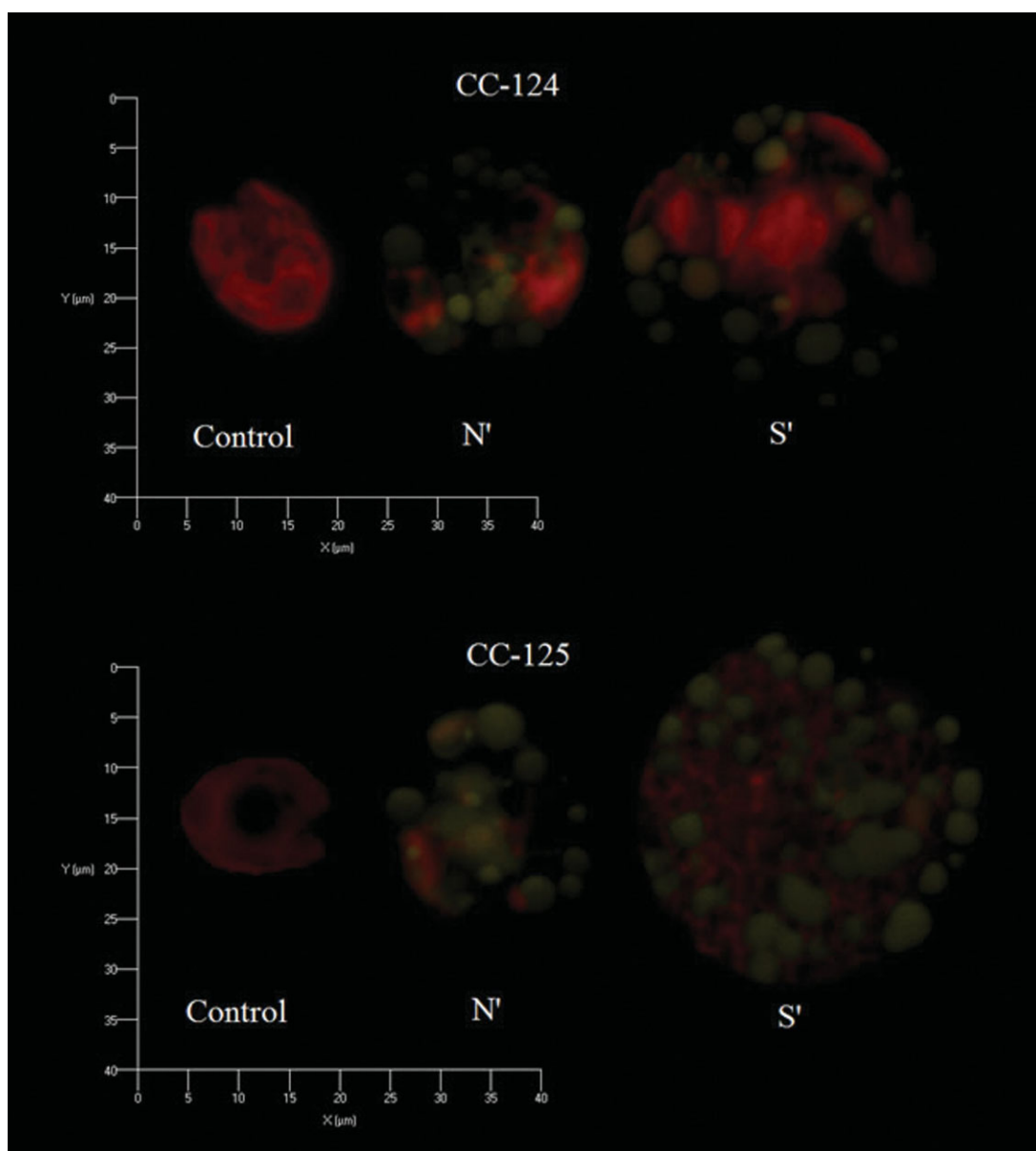


Figure 4. Representative three-dimensional confocal fluorescence microscopy images of 4 days N- or S-starved CC-124 (top) and CC-125 (bottom) strains. Red, chlorophyll autofluorescence; green, Nile Red fluorescence. C, control cells; N', nitrogen-starved cells; S', sulfur-starved cells. [Color figure can be seen in the online version of this article, available at <http://wileyonlinelibrary.com/bit>]

on day 4 was followed by a subsequent decline. Clearly S starvation caused higher TAG accumulation in both strains at the end of 7 days of nutrient starvation. It is generally accepted that algae acclimate to environmental conditions by alteration of their lipid metabolism and composition (Thompson, 1996). Under nutrient deprivation, particularly N-deprivation, some algal species were reported to actively synthesize TAG as an efficient carbon sink (Guschina, 2006). It has also been shown that nitrogen limitation increases the C/N ratio, because reduced synthesis of amino acids and proteins leads to storage of an increased portion of carbon in polysaccharides and/or lipids (Dean et al., 2010; Jakob et al.,

2007). While S starvation in microalgae has been analyzed as a potential tool for increasing hydrogen production, to our knowledge, there is no study so far reported on use of S starvation or comparison of S and N starvation on increasing biodiesel feedstock production. Our results, obtained by measuring both lipid and relative TAG contents, clearly demonstrate that S starvation is a better way of increasing biodiesel feedstock production than N starvation.

In order to determine the levels of carbohydrate structures, both oligosaccharide and polysaccharide peaks were analyzed. Relative increment of oligosaccharide content was higher in S-starved cells than those of N-

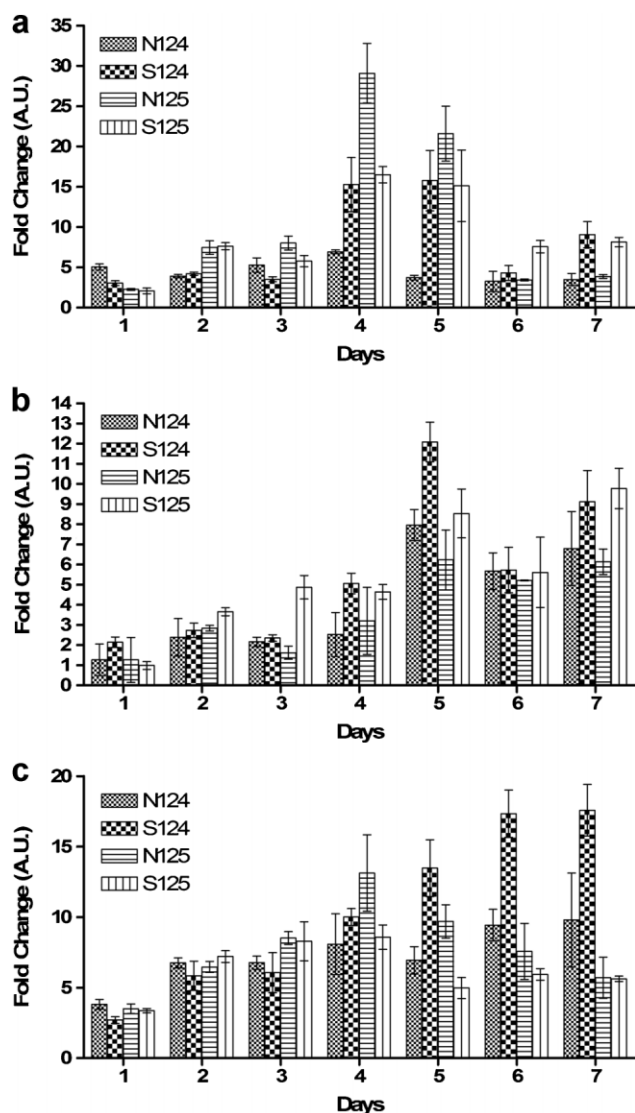


Figure 5. Changes in TAG:amide I ratio (a), oligosaccharide:amide I ratio (b) and carbohydrate:amide I ratio within CC-124 and CC-125 strains in response to N or S deprivation. For all data sets, each point is the mean (\pm SE) of at least three FTIR spectra from pooled samples (derived from triplicate flasks). Each of the spectra was separately derived from randomly selected small groups of cells. Ratios of TAG, carbohydrate and oligosaccharides to amide I of control samples were arbitrarily assigned a value of 1, independently for each time point. Thus, comparisons of changes between different time points are not possible in this representation. C124 and C125 indicate control cells, N124 and N125 indicate N-starved cells, S124 and S125 indicate S-starved CC-124 and CC-125 cells, respectively.

starved ones. The ratio of oligosaccharide to amide I showed a gradual increase in N- and S-starved CC-125 strains, increasing from an initial value of 1.2–0.9 to a final value of 6.3–9.8 during 7 days of nutrient starvation (Fig. 5b). However, in both N- and S-starved CC-124 cells, the ratio increased up to 7.9–12.9 on day 5 and was relatively constant afterwards, with values of 6.8–9.1 at the end of 7th day of nutrient starvation (Fig. 5b).

Land plants and algae produce specific molecules in response to attack by pathogens or to abiotic stress such as nutrient deprivation. Proteins, lipids, or oligosaccharides induce localized or systemic resistance. Oligosaccharides were described as regulatory molecules biologically active at very low concentrations (nM) and were called elicitors (Albersheim et al., 1992). During the past two decades, oligosaccharides were studied for their action on growth regulation, development, elicitation of defense systems against biotic or abiotic stress (such as nutrient limitation) in plants and algae (Courtois, 2009). Considering that the first day increase in oligosaccharide content was small and this increase gradually accumulated in response to nutrient starvation, our results suggest that oligosaccharide level may play a remarkable role on regulation of carbon storage compounds as polysaccharide or lipid structure.

Sulfur starvation-based relative polysaccharide increase was higher in CC-124 compared to N starvation. Relative polysaccharide content gradually increased in N- and S-starved CC-124 strains, increasing from an initial value of 3.8–2.7 to a final value of 9.8–17.6 (Fig. 5c) during 7 days of nutrient starvation. On the other hand, gradual increase in relative polysaccharide level reached its maximum level with a value of 13.1–8.6 on day 4 and this increase was followed by a subsequent decline, reaching a value of 5.7–5.6 on day 7 in N- and S-starved CC-125 cells. Carbohydrate and lipids are two major carbon and energy storage compounds occurring in many plant and microalgal cells, particularly under stress conditions. Lipid and carbohydrate synthesis pathways are well studied; however, possible interactions between the two pathways during nutrient starvation are less understood. Both fluorescence and infrared spectroscopy results show that the increase in carbohydrate level was fast and aggressive in response to nutrient starvation. Moreover, fluorescence spectrometric measurement showed that maximum increase in starch content was threefold higher than the lipid content increment. Finally, considering continuous increase in oligosaccharide content starting from first day of nutrient starvation, we hypothesize that changes in oligosaccharide levels may have an important role in directing carbon structure storage as lipid or carbohydrate compounds in a proportional ratio.

Conclusions

Recently, the applicability of FTIR spectroscopy for the quantification of cellular amounts of macromolecules or elemental ratios has been studied (Wagner et al., 2010). Our study shows that the use of FTIR is a reliable method for quantitative measurement of biological macromolecules. The FTIR results were supported by fluorescence spectrometric measurements in this study. The most notable difference between *C. reinhardtii* wild-type CC-124 and CC-125 strains is that CC-124 carries the *agg1* allele for photoactive aggregation while CC-125 carries *agg1+* allele at this locus. Our results suggest that mating type is an

important factor determining physiological response to mineral deprivation. Wild-type CC-124 and CC-125 strains exhibit different levels of regulation responses under mineral deficiency. Lastly, there are a large number of studies reporting increased hydrogen production using S deprivation (McKinlay and Harwood, 2010) and increasing lipid production via N deprivation (Li et al., 2010). However, to our knowledge, there is no study so far reported on use of S starvation and the comparison of the effects of S and N deprivation in biodiesel feedstock production. Our results showed that 4 days of N or S starvation is a promising way of increasing algal biodiesel feedstock production. However, considering that 4 days of S deprivation leads to an increased total biovolume and stimulates more lipid and carbohydrate accumulation, S starvation seems to be a better way of stimulating biodiesel feedstock production of wild-type *C. reinhardtii* compared to N starvation.

We thank A. Emin Topal for technical assistance and Ayse B. Tekinay for critical reading of the manuscript.

References

- Albersheim P, Darvill A, Augur C, Cheong J, Eberhard S, Hahn M, Marfa V, Mohnen D, Oneill M, Spiro M, York WE. 1992. Oligosaccharins—Oligosaccharide regulatory molecules. *Acc Chem Res* 25(2):77–83.
- Balat M. 2008. Progress in biogas production processes. *Energy Edu Sci Technol* 22:15–35.
- Ball SG, Dirick LÈ, Decq AÈ, Martiat JC, Matagne RÈF. 1990. Physiology of starch storage in the monocellular alga *Chlamydomonas reinhardtii*. *Plant Sci* 66(1):1–9.
- Ball S, Marianne T, Dirick L, Fresnoy M, Delrue B, Decq A. 1991. A *Chlamydomonas reinhardtii* low-starch mutant is defective for 3-phosphoglycerate activation and orthophosphate inhibition of ADP-glucose pyrophosphorylase. *Planta* 185(1):17–26.
- Bligh EG, Dyer WJ. 1959. A rapid method for total lipid extraction and purification. *Can J Biochem Physiol* 37:911–917.
- Bradford MM. 1976. A rapid and sensitive method for the quantitation of microgram quantities of protein utilizing the principle of protein-dye binding. *Anal Biochem* 72:248–254.
- Collins TJ. 2007. ImageJ for microscopy. *Biotechniques* 43(1 Suppl):25–30.
- Converti A, Casazza AA, Ortiz EY, Perego P, Del Borghi M. 2009. Effect of temperature and nitrogen concentration on the growth and lipid content of *Nannochloropsis oculata* and *Chlorella vulgaris* for biodiesel production. *Chem Eng Process* 48(6):1146–1151.
- Courtois J. 2009. Oligosaccharides from land plants and algae: Production and applications in therapeutics and biotechnology. *Curr Opin Microbiol* 12(3):261–273.
- Dean AP, Sigee DC, Estrada B, Pittman JK. 2010. Using FTIR spectroscopy for rapid determination of lipid accumulation in response to nitrogen limitation in freshwater microalgae. *Bioresour Technol* 101(12):4499–4507.
- Degrenne B, Pruvost J, Titica M, Takache H, Legrand J. 2011. Kinetic modeling of light limitation and sulfur deprivation effects in the induction of hydrogen production with *Chlamydomonas reinhardtii*. Part II: Definition of model-based protocols and experimental validation. *Biotechnol Bioeng* 108(10):2288–2299.
- Demirbas A. 2008. Recent progress in biorenewable feedstocks. *Energy Edu Sci Technol* 22:69–95.
- Doan TTY, Sivaloganathan B, Obbard JP. 2011. Screening of marine microalgae for biodiesel feedstock. *Biomass Bioenergy* 35:2534–2544.
- Elsley D, Jameson D, Raleigh B, Cooney MJ. 2007. Fluorescent measurement of microalgal neutral lipids. *J Microbiol Methods* 68(3):639–642.
- Guschina IA, Harwood JL. 2006. Lipids and lipid metabolism in eukaryotic algae. *Prog Lipid Res* 45:160–186.
- Harris EH. 1989. *The Chlamydomonas sourcebook: A comprehensive guide to biology and laboratory use*. San Diego: Academic Press. xiv, pp 780.
- Hsieh CH, Wu WT. 2009. Cultivation of microalgae for oil production with a cultivation strategy of urea limitation. *Bioresour Technol* 100(17):3921–3926.
- Jakob T, Wagner H, Stehfest K, Wilhelm C. 2007. A complete energy balance from photons to new biomass reveals a light- and nutrient-dependent variability in the metabolic costs of carbon assimilation. *J Exp Bot* 58(8):2101–2112.
- Jeffrey S, Humphrey GF. 1975. New spectrophotometric equations for determining chlorophylls a, b, c1 and c2 in higher plants, algae and natural phytoplankton. *Biochem Physiol Pflanz* 167(19):1–194.
- Klut ME, Stockner J, Bisalputra T. 1989. Further use of fluorochromes in the cytochemical characterization of phytoplankton. *Histochem J* 21(11):645–650.
- Kruse O, Rupprecht J, Mussnug JH, Dismukes GC, Hankamer B. 2005. Photosynthesis: A blueprint for solar energy capture and biohydrogen production technologies. *Photochem Photobiol Sci* 4(12):957–970.
- Ledford H, Niyogi K. 2005. Singlet oxygen and photo-oxidative stress management in plants and algae. *Plant Cell Environ* 28(8):1037–1045.
- Li Y, Han D, Hu G, Sommerfeld M, Hu Q. 2010. Inhibition of starch synthesis results in overproduction of lipids in *Chlamydomonas reinhardtii*. *Biotechnol Bioeng* 107(2):258–268.
- Lichtenthaler H. 1987. Chlorophylls and carotenoids: Pigments of photosynthetic biomembranes. *Methods enzymol* 148(2):350–382.
- Liu ZY, Wang GC, Zhou BC. 2008. Effect of iron on growth and lipid accumulation in *Chlorella vulgaris*. *Bioresour Technol* 99(11):4717–4722.
- Lynn S, Kilham S, Kreeger D, Interlandi S. 2000. Effect of nutrient availability on the biochemical and elemental stoichiometry in the freshwater diatom *Stephanodiscus minutulus* (Bacillariophyceae). *J Phycol* 36(3):510–522.
- Marshall WF. 2008. Basal bodies: Platforms for building cilia. *Curr Topics Dev Biol* 85:1–22.
- McKinlay J, Harwood C. 2010. Photobiological production of hydrogen gas as a biofuel. *Curr Opin Biotechnol* 21(3):244–251.
- Merchant SS, Prochnik SE, Vallon O, Harris EH, Karpowicz SJ, Witman GB, Terry A, Salamov A, Fritz-Laylin LK, Maréchal-Drouard L, et al. 2007. The *Chlamydomonas* genome reveals the evolution of key animal and plant functions. *Science* 318(5848):245–250.
- Moazami N, Ranjbar R, Ashori A, Tangestani M, Nejad A. 2011. Biomass and lipid productivities of marine microalgae isolated from the Persian Gulf and the Qeshm Island. *Biomass Bioenergy* 35(5):1935–1939.
- Moellering ER, Benning C. 2010. RNA interference silencing of a major lipid droplet protein affects lipid droplet size in *Chlamydomonas reinhardtii*. *Eukaryot Cell* 9(1):97–106.
- Morsy FM. 2011. Acetate versus sulfur deprivation role in creating anaerobiosis in light for hydrogen production by *Chlamydomonas reinhardtii* and *Spirulina platensis*: Two different organisms and two different mechanisms. *Photochem Photobiol* 87(1):137–142.
- Movasaghi Z, Rehman S, Rehman I. 2008. Fourier transform infrared (FTIR) spectroscopy of biological tissues. *Appl Spectrosc Rev* 43(2):134–179.
- Rochaix JD. 2002. *Chlamydomonas*, a model system for studying the assembly and dynamics of photosynthetic complexes. *FEBS Lett* 529(1):34–38.
- Rodolfi L, Chini Zittelli G, Bassi N, Padovani G, Biondi N, Bonini G, Tredici MR. 2009. Microalgae for oil: Strain selection, induction of lipid synthesis and outdoor mass cultivation in a low-cost photobioreactor. *Biotechnol Bioeng* 102(1):100–112.

- Thompson G. 1996. Lipids and membrane function in green algae. *Biochim Biophys Acta* 1302(1):17–45.
- Wagner H, Liu Z, Langner U, Stehfest K, Wilhelm C. 2010. The use of FTIR spectroscopy to assess quantitative changes in the biochemical composition of microalgae. *J Biophotonics* 3(8–9):557–566.
- Wang ZT, Ullrich N, Joo S, Waffenschmidt S, Goodenough U. 2009. Algal lipid bodies: Stress induction, purification, and biochemical characterization in wild-type and starchless *Chlamydomonas reinhardtii*. *Eukaryot Cell* 8(12):1856–1868.
- Weis VM, Verde EA, Reynolds WS. 2002. Characterization of a Short form peridinin chlorophyll protein (PCP) cDNA and protein from the symbiotic dinoflagellate *Symbiodinium muscatinei* (Dinophyceae) from the sea anemone *Anthopleura elegantissima* (Cnidaria) 1. *J Phycol* 38(1):157–163.
- Work V, Radakovits R, Jinkerson R, Meuser J, Elliott L, Vinyard D, Laurens L, Dismukes G, Posewitz M. 2010. Increased lipid accumulation in the *Chlamydomonas reinhardtii* sta7-10 starchless isoamylase mutant and increased carbohydrate synthesis in complemented strains. *Eukaryot Cell* 9(8):1251–1261.
- Young EB, Beardall J. 2003. Photosynthetic function in *Dunaliella tertiolecta* (Chlorophyta) during a nitrogen starvation and recovery cycle. *J Phycol* 39(5):897–905.
- Zemke P, Wood B, Dye D. 2010. Considerations for the maximum production rates of triacylglycerol from microalgae. *Biomass Bioenergy* 34(1):145–151.
- Zhang L, Happe T, Melis A. 2002. Biochemical and morphological characterization of sulfur-deprived and H₂-producing *Chlamydomonas reinhardtii* (green alga). *Planta* 214:552–561.